June 2019

Reconstruction of Radar Images by Using Spherical Mean and Regular Radon Transforms

Ozan Pirbudak
University of South Florida, opirbudak@mail.usf.edu

Reconstruction of Radar Images by Using Spherical Mean and Regular Radon Transforms

by

Ozan Pirbudak

A thesis submitted in partial fulfillment
of the requirements for the degree of
Master of Arts
Department of Mathematics & Statistics
College of Arts and Sciences
University of South Florida

Major Professor: Razvan Teodorescu, Ph.D
Sherwin Kouchekian, Ph.D
Wen-Xiu Ma, Ph.D

Date of Approval: June 5th, 2019

Keywords: Inverse Problems, Integral Transforms, Radon Transform, Attenuation Correction, QPE

Dedication

This work is dedicated to my family…

Acknowledgment

First, I would like to express my gratitude to my major advisor, Dr. Razvan Teodorescu for his support, feedback, excellent guidance and endless patience. Whenever I needed him, he was around me all the time. Thank you for playing a vital role in the completion of this thesis. I could not achieve this without your support.

I am also grateful to my committee members, Dr. Sherwin Kouchekian and Dr. Wen-Xiu Ma for their valuable guidance, feedback, and encouragement.

I would also like to thank Dr. Özge Özel whose love, support and encouragement have motivated me to finish my thesis. Additionally, I would like to thank my friend Sarper Demirdöğen for collecting many memories in the U.S.

Moreover, I would like to thank Dr. Kurtuluş Öztürk, Cüneyt Geçer and Erdem Erdi for their support and help to start this graduate journey.

Last but not least, I take this opportunity to express gratitude to Turkish State Meteorological Service for providing me with the scholarship to study in the U.S. A special note of gratitude also goes to Mustafa Kemal Ataturk who established Turkish Republic and initiated this scholarship.

Table of Contents

List of Tables

List of Figures

Abstract

The goal of this study is the recovery of functions and finite parametric distributions from their spherical means over spheres and designing a general formula or algorithm for the reconstruction of a function f via its spherical mean transform. The theoretical study is and supported with anumerical implementation based on radar data. In this study we approach the reconstruction problem in two different way. The first one is to show how the reconstruction problem could be converted to a Prony-type system of equations. After solving this Prony-type system of equations, one can extract the parameters that describe the corresponding functions or distributions efficiently. The second way is to solve this problem via a backprojection procedure.

Chapter 1

The Inverse Transform Problem

1.1 Overview

Given a function h on $\mathbb{R}^+ = [0, \infty)$ and a fixed integer $n > 0$, the problem is to recover *signals* $f : \mathbb{R}^n \to \mathbb{R}$ of the form

$$f(y) = \sum_{i=1}^{k} a_i h(|y - y_i|), y_i \in \mathbb{R}^n, a_i \in \mathbb{R}\backslash\{0\}, \quad 1 \leq i \leq k, \tag{1.1}$$

from the spherical mean transform. We also recover the signals f of the form

$$f(y) = \sum_{i=1}^{k} a_i \delta_{y_i}(y), y_i \in \mathbb{R}^n, a_i \in \mathbb{R}\backslash\{0\}, \quad 1 \leq i \leq k, \tag{1.2}$$

where δ_{y_i} is the delta function supported at y_i. We also examine the case when the support of f consists not only of points, but also hyperplanes.

Functions and measures of the types (1.1) and (1.2) are used in various scientific areas, such as computerized tomography, bio-imaging, signal processing [6, 24, 25] and in a variety of mathematical areas like integral geometry, inverse problems, and approximation theory [3, 7, 23, 28]. Specifically, the problem discussed here is finding a general formula or algorithm to reconstruct a function f on $\mathbb{R}^n$, from its spherical mean transform.

Since every sphere in $\mathbb{R}^n$ is characterized by its center point $s \in \mathbb{R}^n$ and radius $0 \leq r$, the set of all spheres in $\mathbb{R}^n$ is $n + 1$ dimensional. Thus, the reconstruction problem from spherical means is overdetermined, since $\mathbb{R}^n$ is n dimensional. Hence, a restriction of the domain of definition of the spherical mean transform has to be implemented to arrive at a well-posed problem. Generally, the spherical mean transform is restricted to a set of the form $\Gamma \times \mathbb{R}^+$, where Γ is a hypersurface in $\mathbb{R}^n$, as an assumption.

The reconstruction problem for a function from spherical mean transform (SMT) which is restricted to such family of sets shows up in various useful areas such as hybrid imaging tomography (thermoacoustic and photoacoustic), radar imaging, integral geometry, inverse problem for PDE, and approximation

theory [1–3, 6, 9, 10, 15, 16, 31, 36]. During the last century, the problem of reconstructing a function from its SMT was studied in different cases where Γ is a quadratic hyper surface [2, 9, 10, 15, 16, 21], a plane [5], or a cylinder [36]. In all of the above attained results, except for some smoothness and support conditions, there is no assumption that these functions need to be recovered. However, as all the functions considered are of the form (1.1), they can be indexed by a finite set of parameters. Therefore, to gain a well-posed problem, we need to restrict the set Γ to a discrete subset [31].

REMARK 1 Since every function f of the form (1.1) depends on finite set of parameters, it should be observed that the set $\Gamma \times \mathbb{R}^+$ is one dimensional,where Γ is discrete. It should also be observed that the discrete set of radii could not be restricted. On the contrary, reconstruction procedure of the function f may change based on the function h. Since the set of radii is discrete, it can be said that the sphere set defined on spherical mean transform is at most countable. For this situation, choosing a small enough function h whose support is close to the origin, and any of the spheres of the integration not intersecting the support of f, it is impossible to reconstruct the function f [31].

The results of this study suggest that the reconstruction of a signal f of the form (1.1) or (1.2) is possible if the set Γ of centers of the spheres of integration comprises sufficiently many points. The main point of these results is to convert the reconstruction problem to a nonlinear Prony's type system of equations. In order to solving the Prony's system, it is assumed that the amplitudes of f at $y_1, ..., y_s$, are mutually distinct. Thus, the solutions to the Prony's system's could be used to obtain information about distances between the points in Γ and the translations $z_1, ..., z_s$ [31, p.438]. Based on this information, one can obtain the points $y_1, ..., y_s$ and the amplitudes $z_1, ..., z_s$ that describe the signal f.

In this study, we first give a brief description for spherical mean transform generally for distributions and start to reconstruct signals of the form (1.2). Then we indicate how to modify the reconstruction method for recovering signals of the form (1.1).Additionally, we will discuss how to reduce the spherical mean transform to a regular Radon transform and then give a numerical implementation by using captured radar images. In the last chapter, we will discuss the Regional Attenuation Correction using Radon transform and two reconstruction techniques.

Chapter 2

Integral Mean Transforms

2.1 Mathematical Background

Let $\mathbb{R}^n$ be the n dimensional Eucledian space, $\mathbb{S}^{n-1}$ is the unit sphere in $\mathbb{R}^n$, and $\mathbb{R}^+$ is the ray [0,∞). Let $\mathbb{S}_{\varphi}^{n-2}$ be $n-2$ dimensional great subsphere in $\mathbb{S}^{n-1}$ that is perpendicular to φ where $\varphi \in \mathbb{S}^{n-1}$:

$$\mathbb{S}_{\varphi}^{n-2} = \{\gamma \in \mathbb{S}^{n-1} : \gamma \cdot \varphi = 0\}$$

where $\cdot$ is the usual scalar product on $\mathbb{R}^n$.

Let j_α be the normalized Bessel function, that is $j_\alpha(\theta) = \theta^{-\alpha} J_\alpha(\theta)$, where J_α is the Bessel function:

$$J_\alpha = \sum_{i=0}^{\infty} \frac{(-1)^i}{i!\Gamma(i+\alpha+1)} (\frac{s}{2})^{2i+\alpha} \text{ for every order } \alpha \geq 0$$

Let C_m^θ be the Gegenbauer polynomial of order $\theta > 0$ and non-negative degree m on [-1,1] :

$$C_m^\theta(s) = \sum_{0 \leq i \leq \frac{m}{2}} \frac{(-1)^i \Gamma(\theta+m-i)}{i!(m-2i)!\Gamma(\theta)} (2s)^{m-2i}.$$

For $\theta = 0$, this polynomial intersect with the Chebyshev polynomial denoted by T_m :

$$C_m^0(s) = T_m(s) := cos(m\ arccos(s)).$$

By [35] for every $\theta \geq 0, \{C_m^\theta\}_{m=0}^{\infty}$ is orthogonal with respect to the

$$< f, h >= \int_{-1}^{1} f(s)h(s)(1-s^2)^{\theta-\frac{1}{2}} ds \text{ on } C[-1,1]$$

where f, h are continuous on $[-1,1]$, and the Gegenbauer Polynomial also satisfies the following relations :

$$\int_{-1}^{1} C_m^\theta(s) C_n^\theta(s)(1-s^2)^{\theta-\frac{1}{2}} ds = 0, \quad m \neq n$$

$$\int_{-1}^{1}(C_m^{\theta}(s))^2(1-s^2)^{\theta-\frac{1}{2}}ds = \frac{2^{1-2\theta}\pi\Gamma(m+2\theta)}{m!(\theta+m)(\Gamma(\theta))^2}$$

Let $C(\mathbb{R}^n)$ and $C(\mathbb{R}^+)$ be the sets of continuous real functions on $\mathbb{R}^n$ and $\mathbb{R}^+$ respectively with the following inner products

$$< f, h >_{\mathbb{R}^n} = \int_{\mathbb{R}^n} f(a)h(a)da$$

$$< f, h >_{\mathbb{R}^+} = \int_{\mathbb{R}^+} f(b)h(b)db$$

where the integrals converge. For $a_0 \in \mathbb{R}^n, \gamma \in \mathbb{S}^{n-1}$ and $\tau > 0$, define the following distribution on $C(\mathbb{R}^n)$

$$\delta_{a_0}(f) = f(a_0)$$

$$\delta_{(\gamma,\tau)}(f) = \int_{a\cdot\gamma=\tau} f(a)d_{m_a}$$

DEFINITION 2.1.1 *[31] The spherical mean transform at a given point $x \in \mathbb{R}^n$ can be defined as the following*

$$R_x : C(\mathbb{R}^n) \to C(\mathbb{R}^+)$$

$$R_x(f)(s) = s^{n-1}\int_{|\gamma|=1} f(x+s\gamma)d\gamma, s \geq 0$$

Say $f \in C(\mathbb{R}^n)$ and $\lambda \in C(\mathbb{R}^+)$, then

$$< R_x f, \lambda >_{\mathbb{R}^+} = \int_0^{\infty} R_x(f)(s)\lambda(s)ds = \int_0^{\infty} s^{n-1}\int_{|\gamma|=1} f(x+s\gamma)d\gamma\lambda(s)ds$$

Take $x + s\gamma = y$ and $dy = s^{n-1}d\gamma d(s)$, then

$$< R_x f, \lambda >_{\mathbb{R}^+} = \int_{\mathbb{R}^n} f(y)\lambda(|x-y|)dy =< f, \lambda(|x-y|) >_{\mathbb{R}^n}$$

Hence, we define the dual spherical mean transform at x

$$R_x^* : C(\mathbb{R}^+) \to C(\mathbb{R}^n)$$

$$R_x^*(\lambda)(y) = \lambda(|x-y|)$$

DEFINITION 2.1.2 *[31] For a given point $x \in \mathbb{R}^n$ and distribution $T : C(\mathbb{R}^n) \to \mathbb{R}$, the Spherical mean transform R_x of T is :*

$$R_xT : C(\mathbb{R}^+) \to \mathbb{R}$$

$$(R_xT)(\lambda) = T(R_x^*\lambda) = T(\lambda(|x - \cdot|))$$

By Definition 2.2, if we take $T = f \in C(\mathbb{R}^n)$, then the spherical mean transform at $x \in \mathbb{R}^n$ is:

$$(R_xf)(\lambda) = \int_{\mathbb{R}^n} f(y)\lambda(|x - y|)dy, \lambda \in C(\mathbb{R}^+)$$

THEOREM 2.1 *[31, p.442] Let $f : C(\mathbb{R}^n) \to R$ be a distribution of*

$f = \sum_{k=1}^m a_k\delta_{x_k}$ $x_i \in \mathbb{R}^n, a_i \in \mathbb{R}\{0\}$ $1 \le i \le m$ *where m is a positive integer such that $x_i \neq x_j$ and $a_i \neq a_j, 1 \le i < j \le m$.*

Suppose that spherical mean transform of f is given at $\frac{1}{2}(n \cdot m(m-1) + 2n + 2)$ points such that there is no hyperplane in $\mathbb{R}^n$. Then, the points $x_1, ..., x_m$ and the amplitudes $a_1, ..., a_m$ can be uniquely recovered.

Proof. Let Γ be the set of points on which the spherical mean transform of given f. For $\forall y \in \Gamma$ and $h_l \in C(\mathbb{R}^+)$, where $h_l(s) = s^l (s \in \mathbb{N} \bigcup 0)$.

$$(R_yf)(h_l) = f(R_y^*h_l) = f(h_l(|y - \cdot|)). \text{ (by definition 2.2)}$$

$$= \sum_{k=1}^m a_k\delta_{x_k}(h_l(|y - \cdot|))$$

$$= \sum_{k=1}^m a_k(h_l(|y - x_k|))$$

$$= \sum_{k=1}^m a_k|y - x_k|^l$$

Say $\tau_l = (R_yf)(h_l),\ 0 \ge l \ge 2m - 1$ then we get,

$$\begin{pmatrix} 1 & 1 & \cdots & 1 \\ |y-x_1| & |y-x_2| & \cdots & |y-x_m| \\ |y-x_1|^2 & |y-x_2|^2 & \cdots & |y-x_m|^2 \\ \vdots & \vdots & \cdots & \vdots \\ |y-x_1|^{2m-1} & |y-x_2|^{2m-1} & \cdots & |y-x_m|^{2m-1} \end{pmatrix} \begin{pmatrix} a_1 \\ a_2 \\ \vdots \\ a_m \end{pmatrix} = \begin{pmatrix} \tau_0 \\ \tau_1 \\ \vdots \\ \tau_{2m-1} \end{pmatrix} = \bar{\tau} \qquad (2.1)$$

This system is of Prony's type where $z_i = |y - x_i|$ and $a_i \neq 0, i = 1, 2, ..., m$ can be solved as seen below :

Define a polynomial

$$p(z) = z^{m+1} + \sum_{k=0}^{m-1} v_k z^{m-k}$$

and consider coefficient vector

$$p^{m-1} = [p_0, ..., p_{m-1}]^T.$$

This coefficients can be determined from $\bar{\tau}$. To finish this, form the matrix from $p^{(m)}$ is as follows:

$$\begin{pmatrix} p_0 & \cdots & p_{m-1} & 1 & \cdots & 0 \\ & \ddots & & \ddots & \ddots & \\ 0 & & p_0 & \cdots & p_{m-1} & 1 \end{pmatrix}$$

From the definition of $p(z)$, $v_k \cdot \bar{\tau} = 0$ can be written as follows :

$$\begin{pmatrix} \tau_0 & \tau_1 & \cdots & \tau_{m-1} \\ \tau_1 & \tau_2 & \cdots & \tau_m \\ \vdots & \vdots & & \vdots \\ \tau_{m-1} & \tau_m & \cdots & \tau_{2m-2} \end{pmatrix} p^{(m-1)} = - \begin{pmatrix} \tau_m \\ \tau_{m+1} \\ \vdots \\ \tau_{2m-1} \end{pmatrix} \tag{2.2}$$

$K_m p^{m-1} = -k_m$

To solve this equation, we need to show that K_m is invertible.

K_m can be decomposed as $K_m = V_m diag(a_m) V_m^T$, where V_m is the Vandermonde matrix

$$\begin{pmatrix} 1 & 1 & \cdots & 1 \\ z_1 & z_2 & \cdots & z_m \\ z_1^2 & z_2^2 & \cdots & z_m^2 \\ \vdots & \vdots & \cdots & \vdots \\ z_1^{m-1} & z_2^{m-1} & \cdots & z_m^{m-1} \end{pmatrix}$$

By assumption, $a_i \neq 0, i = 1, ..., m, diag(a_m)$ is non-degenerate. Also, V_m is degenerate iff there are two different indices $1 \leq i, j \leq m$ such that $|y - x_i| = |y - x_j|$ which means y has same distance from x_i and x_j.

Claim: There exists $n + 1$ points $y_1, ..., y_{n+1} \in \Gamma$ such that $\forall\ 1 \leq l \leq n + 1$ the following condition holds:

$$|y_l - x_i| \neq |y_l - x_j| \; \forall \; i, j, \; 1 \leq i, j \leq m, i \neq j \tag{2.3}$$

Proof of Claim $\forall \; y \in \Gamma$ satisfy $|y_l - x_i| = |y_l - x_j|$ for $i \neq j$, if and only if y lies in the unique hyperplane $H_{i,j}$ that divides up two equal parts and is orthogonal to $x_i - x_j$ vector. By assumption, there is no hyperplane in Γ contains more than n points, and there are at most $\frac{1}{2}(m-1)m$ such hyperplanes, then there are at least $n+1$ points in Γ that any of them does not lie in any of these hyperplanes, since Γ contains $\frac{1}{2}(n \cdot m(m-1) + 2n + 2)$ distinct points.

Define $\Gamma^{'} \subset \Gamma, \Gamma^{'} = y_1, y_2, ..., y_{n+1}$ such that $\forall y_i \in \Gamma^{'}$ satisfies (2.3).

For $y_1 \in \Gamma^{'}$, build a system of equations same as (2.2).

Without loss of generality, assume $\mu_i = |y_1 - x_i|$. In equation (2.1), say $y = y_1$. Since $|y_1 - x_i| = \mu_i$ and the roots μ_i are distinct, left hand side of the equation is non-degenerate, so $a_1, ..., a_m$ can be extracted.

Now, we extract the points $x_1, ..., x_m$. For this, we need to solve system of equations (2.2) for $\forall 2 \leq l \leq n+1$ and extract the coefficients of the polynomial whose roots are

$$\mu_{1,l}, ..., \mu_{m,l} = |y_l - x_1|, ..., |y_l - x_m|.$$

Since it is not known which root $\mu_{j,l}$ corresponds to each point x_i for $l \geq 2$, we need to check which permutation of the root $\mu_{1,l}, ...\mu_{m,l}$ solves equation(2.1). So, we need to use the following condition to get unique solution: $a_i \neq a_j, i \neq j$.

Assume, there is a permutation of $\mu_{1,l}, ...\mu_{m,l}$ which is the identity, and another permutation x from $\{1, ..., m\}$ to itself, which solves the equation (2.1) and different from the identity

$$\mu_1^{'} = \mu_{x_1,l}, ..., \mu_m^{'} = \mu_{x_m,l}$$

If we substract these two equations , we get

$$\begin{pmatrix} \mu_{1,l} - \mu_{x_1,l} & \mu_{2,l} - \mu_{x_2,l} & \cdots & \mu_{m,l} - \mu_{x_m,l} \\ \mu_{1,l}^2 - \mu_{x_1,l}^2 & \mu_{2,l}^2 - \mu_{x_2,l}^2 & \cdots & \mu_{m,l}^2 - \mu_{x_m,l}^2 \\ \vdots & \vdots & \cdots & \vdots \\ \mu_{1,l}^{2m-1} - \mu_{x_1,l}^{2m-1} & \mu_{2,l}^{2m-1} - \mu_{x_2,l}^{2m-1} & \cdots & \mu_{m,l}^{2m-1} - \mu_{x_m,l}^{2m-1} \end{pmatrix} \begin{pmatrix} a_1 \\ a_2 \\ \vdots \\ a_m \end{pmatrix} = \begin{pmatrix} 0 \\ 0 \\ \vdots \\ 0 \end{pmatrix} \tag{2.4}$$

LEMMA 2.1 *[31, p.448] Suppose for $n \geq 2, \gamma_1, ..., \gamma_n$ are real numbers such that $\gamma_i \neq \gamma_j, i \neq j$ Suppose x is a permutation from $\{1, ..., n\}$ to itself,that is different from the identity. Define*

$$\begin{pmatrix} \gamma_1 - \gamma_{x(1)} & \gamma_2 - \gamma_{x(2)} & \cdots & \gamma_n - \gamma_{x(n)} \\ \gamma_1^2 - \gamma_{x(1)}^2 & \gamma_2^2 - \gamma_{x(2)}^2 & \cdots & \gamma_n^2 - \gamma_{x(n)}^2 \\ \vdots & \vdots & \cdots & \vdots \\ \gamma_1^n - \gamma_{x(1)}^n & \gamma_2^n - \gamma_{x(2)}^n & \cdots & \gamma_n^n - \gamma_{x(n)}^n \end{pmatrix} = A$$

Then, if $y = (y_1, ..., y_n) \in \mathbb{R}^n$ satisfy $Ay^T = 0$, then $\exists i, j, i \neq j$ such that $y_i = y_j$

Proof. [31, p.448] By induction on $n \geq 2$,since x is different from the identity, then for $n = 2, x(1) = 2$ and $x(2) = 1$. Here, $y = (1, 1)$ is in the kernel of A and it has two equal components for different indices.

Assume the induction hypothesis for every m, such that $2 \leq m \leq n - 1$ and prove it for $n \geq 3$. Assume x does not have any fixed point. Indeed, without loss of generality, suppose $x(n) = n$ then the matrix A becomes the following form

$$\begin{pmatrix} \gamma_1 - \gamma_{x(1)} & \gamma_2 - \gamma_{x(2)} & \cdots & \gamma_n - \gamma_{x(n)} & 0 \\ \gamma_1^2 - \gamma_{x(1)}^2 & \gamma_2^2 - \gamma_{x(2)}^2 & \cdots & \gamma_n^2 - \gamma_{x(n)}^2 & 0 \\ \vdots & \vdots & \cdots & \vdots & \vdots \\ \gamma_1^n - \gamma_{x(1)}^n & \gamma_2^n - \gamma_{x(2)}^n & \cdots & \gamma_n^n - \gamma_{x(n)}^n & 0 \end{pmatrix} = \begin{pmatrix} B & \bar{0} \\ * & 0 \end{pmatrix}$$

where B is the top left matrix of A which is (n-1)x(n-1).

If $Ay^T = 0$, then $y = (y_0, *)$ where $y_0 \in \mathbb{R}^{n-1}$ is in the kernel of B. If $x^{'}$ denotes the restriction of x to the set $\{1, ..., n-1\}$, then $x(\{1, ..., n-1\}) = \{1, ..., n-1\}$ since $x(n) = n.x^{'}$ is also different from the identity. Thus, applying the induction to the B, it follows that y_0 has at least two equal components for different indices. Thus, it is also true for y_1. □

By (2.3), $\mu_{i,l} \neq \mu_{j,l}$ if $i \neq j$, and x is different from the identity. Then, all conditions of Lemma are satisfied. Thus, any vector in the kernel of the matrix, which is the left hand side of (4.4) have to have two equal components for different indices. Thus, $a_i = a_j$ for $i \neq j$, contradiction.

Hence we have the all distances $\lambda_{i,l} = |y_l - x_i|, l = 1, ..., n+1$ for each $1 \leq i \leq m$. So, since there is no hyperplane in $\mathbb{R}^{\kappa}$ which contains the point $y_{1,...,y_{n+1}}$, it can be uniquely recovered the points x_i from the data $\lambda_{i,1}, ..., \lambda_{i,n+1}$ □

REMARK 2 For the distribution of the form (3.1), if the recovered amplitudes have the same value, the procedure to extract f that is used in above theorem will not work anymore, since the proof of this theorem uses only n + 1 points which have different distances from each of the nodes $x_i i = 1, ..., m$. In this case we cannot know which roots correspond to each nodes x_i.

Example: Let f_1 and f_2 be distributions for $n = m = 2$

$$f_1 = \delta(x - r_1) + \delta(x - r_2), f_2 = \delta(x - s_1) + \delta(x - s_2),$$

where

$$r_1 = (0, 1), r_2 = (2, -1), s_1 = (0, -1), s_2 = (2, 1)$$

By Theorem (3.1), we can find $n + 1 = 3$ points y_1, y_2, y_3 on the different lines, and it is known that this points have different distances from each nodes that to be wanted to extract, so we could suppose that the spherical mean transform is only given at this points. In this situation, the information received from the spherical mean transform can intersect for the these distributions.

Assume

$$y_1 = (0, 0), y_2 = (2, 0), y_3 = (1, 1)$$

then, y_1, y_2, y_3 are on the different lines and have different distances from r_1, r_2 of f_1 and s_1, s_2 of f_2.

Since,

$$|y_1 - r_1| = |y_1 - s_1|, |y_1 - r_2| = |y_1 - s_2|$$
$$|y_2 - r_1| = |y_2 - s_1|, |y_2 - r_2| = |y_2 - s_2|$$
$$|y_3 - r_1| = |y_3 - s_2|, |y_3 - r_2| = |y_3 - s_1|,$$

the spherical mean transform takes the same information from f_1 and f_2. Thus they cannot be seperated.

THEOREM 2.2 *[31, p.442] Let $f : C(\mathbb{R}^n) \to R$ be a distribution of*

$$f = \sum_{k=1}^{m} a_k \delta_{(\theta_k,\rho_k)}\ \rho_i \in (0,\infty), \theta_i \in \mathbb{S}^{n-1} a_i \in \mathbb{R}\backslash\{0\}\ 1 \le i \le m$$

where m is a positive integer such that $a_i \neq a_j, for 1 \le i < j \le m$, and the hyperplanes $< x, \theta_1 >= \rho_1, ..., < x, \theta_m >= \rho_m$ are all distinct.

Suppose that spherical mean transform of f is given at $n \cdot m(m-1) + 2n + 1$ points such that there is no hyperplane in $\mathbb{R}^n$ which contains more than n of these given points. Then, the parameters $a_1, \rho_1, \theta_1, ..., a_m, \rho_m, \theta_m$ can be uniquely recovered.

Proof. Let Γ be the set of points on which the spherical mean transform of given f. For $\forall y \in \Gamma$ and $h_l \in C(\mathbb{R}^+)$,where $h_l = e^{-lt^2} (l \in \mathbb{N})$, we have

$$(R_y f)(h_l) = f(R_y^* h_l) = f(h_l(|y - \cdot|)).$$

$$= \sum_{k=1}^{m} a_k \delta_{(\theta_k,\rho_k)}(h_l(|y - \cdot|))$$

$$= \sum_{k=1}^{m} a_k \int_{<x,\theta_k>=\rho_k} (h_l(|y - x|))dm_x$$

$$= \sum_{k=1}^{m} a_k \int_{<x,\theta_k>=\rho_k} e^{-l|y-x|^2} dm_x$$

Take $x = y + z, dm_x = dm_z$, then

$$(R_y f)(h_l) = \sum_{k=1}^{m} a_k \int_{z=<x,\theta_k>-<y,\theta_k>=\rho_k-<y,\theta_k>} e^{-l|z|^2} dm_z$$

$$= \sum_{k=1}^{m} a_k \int_{\mathbb{R}^n} e^{-l(z_1^2+...+z_n^2)} dz_1 ... dz_n$$

$$= \sum_{k=1}^{m} a_k e^{-l(z)^2} \int_{\mathbb{R}^{n-1}} e^{-l(z_1^2+...+z_{n-1}^2)} dz_1 ... dz_{n-1}$$

$$= (\frac{\pi}{l})^{\frac{1-n}{2}} \sum_{k=1}^{m} a_k e^{-l|\rho_k - <y,\theta_k>|^2}$$

Now, say $\tau_l = (\frac{\pi}{l})^{\frac{1-n}{2}} (R_y f)(h_l), \gamma_k = e^{-|\rho_k - <y,\theta_k>|^2}, 1 \le l \le 2m$ then we can get as theorem 3.1

$$\begin{pmatrix} \tau_1 & \tau_2 & \cdots & \tau_m \\ \tau_2 & \tau_3 & \cdots & \tau_{m+1} \\ \vdots & \vdots & & \vdots \\ \tau_m & \tau_{m+1} & \cdots & \tau_{2m--1} \end{pmatrix} p^{(m-1)} = - \begin{pmatrix} \tau_{m+1} \\ \tau_{m+2} \\ \vdots \\ \tau_{2m} \end{pmatrix} \tag{2.5}$$

$K_m p^{m-1} = -k_m$

K_m can be decomposed as $K_m = V_1 diag(a_m) V_2$, where V_1, V_2 are the Vandermonde matrices,

$$\begin{pmatrix} \gamma_1 & \gamma_2 & \cdots & \gamma_m \\ \gamma_1^2 & \gamma_2^2 & \cdots & \gamma_m^2 \\ \vdots & \vdots & \cdots & \vdots \\ \gamma_1^m & \gamma_2^m & \cdots & \gamma_m^m \end{pmatrix} = V_1$$

$$\begin{pmatrix} 1 & \gamma_1 & \cdots & \gamma_1^{m-1} \\ 1 & \gamma_2^2 & \cdots & \gamma_2^{m-1} \\ \vdots & \vdots & \cdots & \vdots \\ 1 & \gamma_m^m & \cdots & \gamma_m^{m-1} \end{pmatrix} = V_2$$

Since V_1, V_2 are Vandermonde, and $\gamma_i \neq 0$ for $i = 1, ..., m$, then V_1 or V_2 are degenerate if and only if there are two different indices $i \neq j$ such that $|\rho_i - < y, \theta_i > | = |\rho_j - < y, \theta_j > |$, which means y has the same distance from $< x, \theta_i >= \rho_i$ and $< x, \theta_j >= \rho_j$.

Claim: There exists $2n+1$ points $y_1, ..., y_{2n+1}$ such that for $\forall\ 1 \leq l \leq 2n+1$, the following condition holds:

$$|\rho_i - < y_l, \theta_i > | \neq |\rho_j - < y_l, \theta_j > |, \forall i, j 1 \leq i, j \leq m, i \neq j \tag{2.6}$$

Proof of Claim $\forall y \in \Gamma$ satisfy $|\rho_i - < y, \theta_i > | = |\rho_j - < y, \theta_j > |$ for $i \neq j$ if and only if y lies on one of the hyperplanes

$$< x, \theta_i + \theta_j >= \rho_i + \rho_j$$
$$< x, \theta_i - \theta_j >= \rho_i - \rho_j$$

By assumption, there is no hyperplane in Γ which contains more than n points, and there are at most (m-1)m such hyperplanes, then there are at least 2n+1 points in Γ that any of them does not lie in any of these hyperplane, since Γ contains $n \cdot m(m-1) + 2n + 1$ distinct points.

As in theorem 3.1, define

$\Gamma^{'} \subset \Gamma, \Gamma^{'} = y_1, y_2, ..., y_{2n+1}$ such that $\forall y_i \in \Gamma^{'}$ satisfies (2.6).

For $y_1 \in \Gamma^{'}$, build a corresponding polynomial with roots and system of equation similar as (2.2).

$$\{\gamma_1, ...\gamma_m\} = \{|\rho_1 - < y_1, \theta_1 > |, ..., |\rho_m - < y_1, \theta_m|\}$$

In order to determine amplitudes $a_1, ..., a_m$, we assume

$\gamma_i = |\rho_i - < y, \theta_i > |$,and solve system of equations similar as (2.1), as we did in theorem 3.1.

Now we extract the parameters $\rho_1, \theta_1, ..., \rho_m, \theta_m$.For this,we need to solve system of equations similar as (2.2) for every $2 \leq l \leq 2n+1$ and extract the coefficients of the polynomial whose roots are

$$\{\gamma_{1,l}, ...\gamma_{m,l}\} = \{|\rho_1 - < y_l, \theta_1 > |, ..., |\rho_m - < y_l, \theta_m > |\}.$$

Thus, we can find the distances

$$|\rho_i - < y_l, \theta_1 > |, ..., |\rho_m - < y_l, \theta_m > | \text{ for } \forall y_l \in \Gamma^{'}, 1 \leq l \leq 2n+1.$$

Hence we get

$$|\rho_i - < y_l, \theta_i > |, l = 1, ..., 2n+1, \forall i, 1 \leq i \leq m \tag{2.7}$$

Uniqueness of (2.7): Let $H :< x, \theta_i >= \rho_i$ be a hyperplane. Suppose $\exists H^{'}$ such that every point $y_l, l = 1, ..., 2n+1$ has same distance from H and $H^{'}$. The set of points that have same distance from such hyperplanes is the union of them. Thus, y_l lies in H and $H^{'}$, then at least one of them contains $n+1$ of these points, contradiction. □

THEOREM 2.3 *[31, p.443] Let $f : \mathbb{R}^n \to \mathbb{R}$ be a function of*

$f(x) = \sum_{k=1}^{m} a_k h(|x - x_k|), x_i \in \mathbb{R}^n, a_i \in \mathbb{R}\backslash\{0\}, 1 \leq i \leq m$ *where m is positive integer such that $x_i \neq x_j$ and $a_i \neq a_j$ for $1 \leq i < j \leq m$, h is function on $\mathbb{R}^+$. Suppose that spherical mean transform of f is given at $\frac{1}{2}(n \cdot m(m-1) + 2n + 2)$ points such that there is no hyperplane in $\mathbb{R}^n$ which contains more than n of these given points. Then, the points $x_1, ..., x_m$ and the amplitudes $a_1, ..., a_m$ can be uniquely recovered.*

LEMMA 2.2 *[31, p.447] For a function f that is defined on $\mathbb{R}^+$,its radial extension belongs to the Schwartz space $S(\mathbb{R}^n)$. Then, f and its Hankel transform F are continuously differentiable and belong to $L^1(\mathbb{R}^+, r^{\frac{n-1}{2}})$.*

Proof. Let $h^{'}$ and $H^{'}$ be the radial extensions of h and H, respectively. In spherical coordinates system in $\mathbb{R}^n$, we have

$$\int_{|x|>1} h^{'}(x)|x|^{\frac{-n-1}{2}}dx = \int_1^\infty \int_{\mathbb{S}^{n-1}} h^{'}(r\theta)r^{\frac{n-1}{2}}d\theta dr = \frac{2\pi^{\frac{n}{2}}}{\Gamma(\frac{n}{2})}\int_1^\infty h(r)r^{\frac{n-1}{2}}dr$$

Since radial extension of h belongs to the Schwartz space,then integral in the left hand side converges, hence also integral in the right hand side converges. Since h is bounded on [0,1] (because $h^{'}$ is bounded on the unit disk), then h is in $L^1(\mathbb{R}^+, r^{\frac{n-1}{2}})$.

Let $\bar{h}$ be the Fourier transform of h. Use the spherical coordinates,

$$\bar{h}(\varphi) = \frac{1}{(2\pi)^{\frac{n}{2}}}\int_{\mathbb{R}^n} h^{'}(x)e^{-i<\varphi,x>}dx = \frac{1}{2\pi^{\frac{n}{2}}}\int_0^\infty \int_{\mathbb{S}^{n-1}} h^{'}(r\theta)e^{-ir<\varphi,\theta>}d\theta r^{n-1}dr$$

Take $\varphi = \lambda\phi$ where $\lambda = |\varphi|$ and $\phi = \frac{\varphi}{|\varphi|}$ and use the identity,

$$\int_{\mathbb{S}^{n-1}} e^{-it<\phi,\theta>} = (2\pi)^{\frac{n}{2}} j_{\frac{n}{2}-1}(t)$$

Then,

$$\bar{h}(\lambda\phi) = \int_0^\infty h(r)j_{\frac{n}{2}-1}(\lambda r)r^{n-1}dr = H(\lambda)$$

Thus, $\bar{h}$ is the radial extension of H. Since $\bar{h}$ maps $S(\mathbb{R}^n)$ onto itself and $\bar{h} \in S(\mathbb{R}^n)$, then the same is true for the radial extension of H. Thus, H belongs to $L^1(\mathbb{R}^+, r^{\frac{n-1}{2}})$ from the same points that used for h and $h^{'}$. □

Proof. [Theorem] Let H be the Hankel transform of h of order $\frac{n}{2} - 1$.

$$H(\lambda) = \int_0^\infty h(r)j_{\frac{n}{2}-1}(\lambda r)r^{n-1}dr \ \lambda \geq 0 \tag{2.8}$$

By above lemma, the radial extension of f is in $S(\mathbb{R}^n)$, then f is continuously differentiable and belongs to $L^1(\mathbb{R}^+, r^{\frac{n-1}{2}})$. Hence we can say that

$$h(r) = \int_0^\infty H(\lambda)j_{\frac{n}{2}-1}(\lambda r)\lambda^{n-1}d\lambda, \ r \geq 0$$

By equation (3.2),

$$f(x) = \sum_{k=1}^m a_k \int_0^\infty H(\lambda)j_{\frac{n}{2}-1}(\lambda|x - x_k|)\lambda^{n-1}d\lambda$$

Take the spherical mean transform of f at a point y, we get

$$(Ryf)(t) = \sum_{k=1}^{m} a_k \int_0^\infty H(\lambda)(Ry(j_{\frac{n}{2}-1}(\lambda|\cdot - x_k|)))(t)\lambda^{n-1}d\lambda$$

$$=\sum_{k=1}^{m} a_k \int_0^\infty H(\lambda) \int_{|\theta|=1}(j_{\frac{n}{2}-1}(\lambda|y - x_k + t\theta|))d\theta\lambda^{n-1}d\lambda t^{n-1}$$

Using the identity

$$\int_{|\theta|=1} j_{\frac{n}{2}-1}(\lambda|x + r\theta|)d\theta = (2\pi)^{\frac{n}{2}} j_{\frac{n}{2}-1}(\lambda r)j_{\frac{n}{2}-1}(\lambda|x|)$$

and we get

$$(R_yf)(t) = (2\pi)^{\frac{n}{2}} \sum_{k=1}^{m} a_k \int_0^\infty H(\lambda)j_{\frac{n}{2}-1}(\lambda|y - x_k|)j_{\frac{n}{2}-1}(\lambda t)\lambda^{n-1}d\lambda t^{n-1}$$

Thus,

$$\frac{(R_yf)(t))}{t^{n-1}(2\pi)^{\frac{n}{2}}} = \sum_{k=1}^{m} a_k \int_0^\infty H(\lambda)j_{\frac{n}{2}-1}(\lambda|y - x_k|)j_{\frac{n}{2}-1}(\lambda t)\lambda^{n-1}d\lambda$$

Taking

$$F(\lambda) = (\sum_{k=1}^{m} a_k j_{\frac{n}{2}-1}(\lambda|y - x_k|))H(\lambda)$$

Then,

$$\frac{(R_yf)(t))}{t^{n-1}(2\pi)^{\frac{n}{2}}} = \int_0^\infty F(\lambda)j_{\frac{n}{2}-1}(\lambda t)\lambda^{n-1}d\lambda \tag{2.9}$$

Here, the right hand side of equation is Hankel transform for F. It is needed to show that F is continuously differentiable and belongs to $L^1(\mathbb{R}^+, r^{\frac{n-1}{2}})$ to use inverse of the Hankel transform of F.

Since H is continuosly differentiable and belongs to $L^1(\mathbb{R}^+, r^{\frac{n-1}{2}})$, then it is also valid for F. Thus, the inverse of Hankel transform of F can be taken as following :

$$\frac{1}{(2\pi)^{\frac{n}{2}}} \int_0^\infty (R_yf)(t)j_{\frac{n}{2}-1}(\lambda t)dt = (\sum_{k=1}^{m} a_k j_{\frac{n}{2}-1}(\lambda|y - x_k|))H(\lambda) \tag{2.10}$$

If we divide both sides with $H(\lambda)$ and take the derivative $2k$ times for $\lambda = 0$,we get

$$\frac{2^{2k-1}(-1)^k k!\Gamma(\frac{n}{2}+k)}{\pi^{\frac{n}{2}}(2k)!}(\frac{1}{H(\lambda)}\int_0^\infty (R_y f)(t) j_{\frac{n}{2}-1}(\lambda t)dt)^{(2k)}|_{\lambda=0}$$

$$\sum_{k=1}^{m} a_k |y - x_k|^{2k} \tag{2.11}$$

By using same procedure in Theorem (3.1) and replacing points y in (2.11) for $k = 0, ..., 2m-1$, we can recover the $x_1, ..., x_m, a_1, ..., a_m$. □

2.2 Reducing Spherical Mean to Regular Radon Transform

Spherical Mean Transform operator R_x (see definition 2.1) transfers all the known properties of the function on R_n,which include the classical hyperplane Radon function and inversion formulas, to R_x. In ths circumstance, λ-cosine transforms and Semyanisty's fractional integrals [29, 30, 33] can be envoked to apply this transition. The Radon transform is a particular case of these integrals [30].

$C^\lambda = V_{a,\lambda} R^\lambda U_{a,\lambda}$ where $V_{a,\lambda}$ and $U_{a,\lambda}$ are certain bijections.

2.2.1 The λ-cosine Transform

Let the SMT of a continuous function f on S^n be

$$(Rf)(x) = \frac{1}{t_{n-1}} \int_S^n f(\mu) d_x \mu \qquad x \in S^n$$

In many cases, it is appropriate to consider the SMT as a member of the normalized cosine transform

$$(C^\lambda f)(x) = \tau_{n,x} \int_{S^n} f(\mu) |x\mu|^\lambda d_* \mu,$$

where $d_*\mu = \frac{d\mu}{t_n}$, $\qquad Re\lambda > -1 \qquad \lambda \neq 0, 2, 4, ..., \qquad \tau_{n,\lambda} = \dfrac{\pi^{\frac{1}{2}}\Gamma(\frac{-\lambda}{2})}{\Gamma(\frac{n+1}{2})\Gamma\frac{(1+\lambda)}{2}}$

2.2.2 Radon Transform

The Radon Transform of the function $f(x, y) x, y \in R$ is defined as following

$$g(\rho, \theta) = (Rf)(\rho, \theta) = \int_{-\infty}^{\infty}\int_{-\infty}^{\infty} f(x, y)\delta(\rho - xcos\theta - ysin\theta)dxdy,$$

where $\delta(\cdot)$ is the Dirac Delta function.

The plot of the Radon transform is referred to as a sinogram from its sinusoid shape. The inverse Radon transform is applied to the image to recover the image from sinogram. There are many inversion formulas for the Radon transform.*The filtered back projection* is the most commonly used technique. It is derived as follows

$$f(x,y) = \int_{-\infty}^{\infty}\int_{-\infty}^{\infty} F(u,v)e^{-2\pi i(ux+vy)}dudv$$

and changing variables to polar coordinates

$u = wcos\theta, v = wsin\theta, dudx = wdwd\theta$

Then,

$$f(x,y) = \int_{0}^{2\pi}\int_{0}^{\infty} wF(wcos\theta, wsin\theta)e^{-2\pi wi(xcos\theta+ysin\theta)}dwd\theta$$

$$= \int_{0}^{\pi}\int_{-\infty}^{\infty} |w|F(wcos\theta, wsin\theta)e^{-2\pi wi(xcos\theta+ysin\theta)}dwd\theta$$

$$= \int_{0}^{\pi}\int_{-\infty}^{\infty} |w|(\int_{-\infty}^{\infty} t_\theta(\rho)e^{2\pi i\rho w})e^{-2\pi wi(xcos\theta+ysin\theta)}dwd\theta$$

The last equation above can be seperated as two steps. The following first part is filtering step in the frequency domain

$$\hat{t}_\theta(\rho) = \int_{-\infty}^{\infty} |w|(\int_{-\infty}^{\infty} t_\theta(\rho)e^{2\pi i\rho w})e^{-2\pi\rho wi}dw$$

and the rest is followed by projection step

$$\hat{g}(\rho,\theta) = \hat{t}_\theta(\rho)$$

$$f(x,y) = \int_{0}^{\pi} \hat{g}(xcos\theta + ysin\theta, \theta)d\theta$$

$$= \int_{0}^{\pi}\int_{-\infty}^{\infty} \hat{g}(\rho,\theta)\delta(\rho - xcos\theta - ysin\theta)d\rho d\theta$$

Here $\hat{g}(\rho,\theta)$ is called *filtered backprojection*.

2.3 Numerical Implementation

In this section, a reconstructed Modified Shepp-Logan phantom and a reconstructed captured radar image were given. The codes were built in MATLAB and given in the Appendix A. Reconstruction period was around 10 seconds. Different discretization number were implemented and results showed that while increasing the discretization number, image resolutions increase.

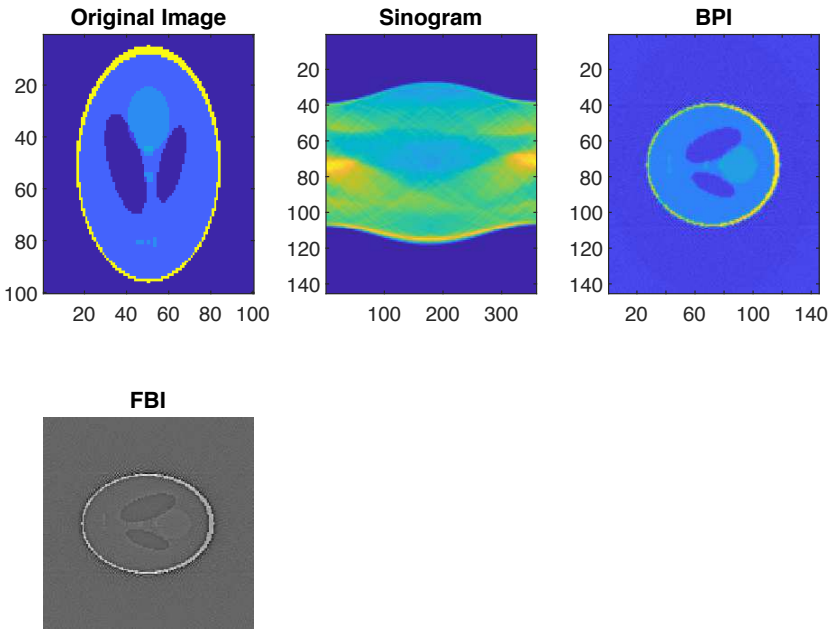

Figure 1.: Reconstruction for Modified Shepp-Logan Image

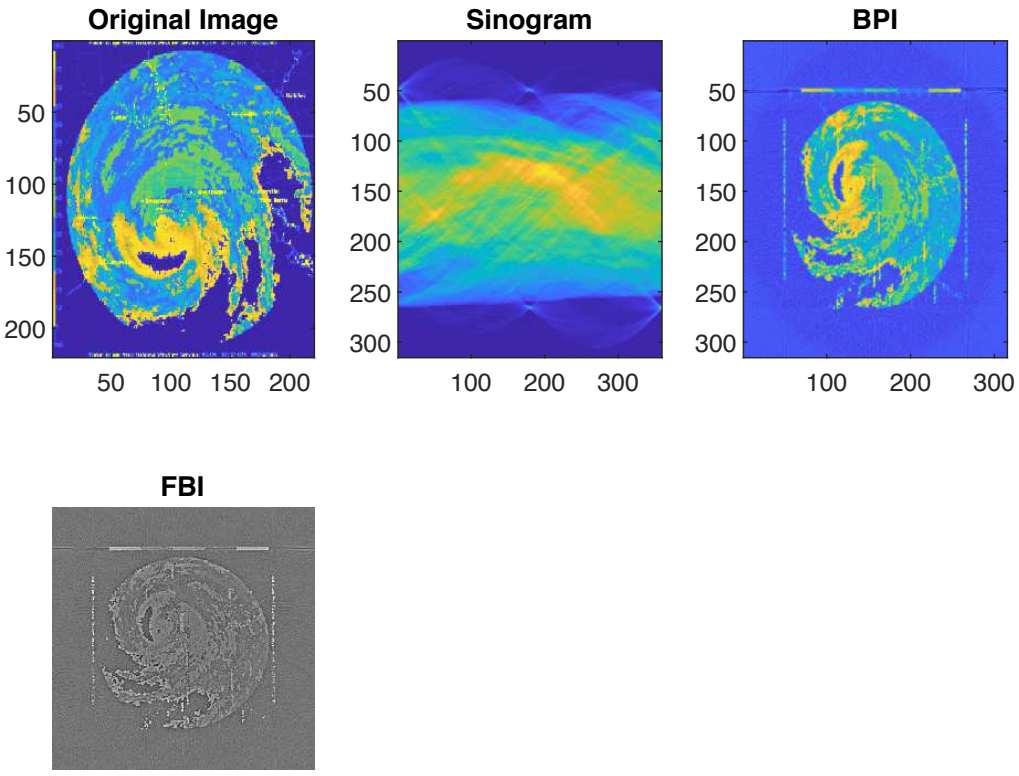

Figure 2.: Reconstruction for Captured Weather Radar Image

Chapter 3

Regional Attenuation Correction

Correction of echo attenuation is challenging, since the variation of the raindrop size distribution affects the accuracy of precipitation quantitative estimates. Since microwave links can accurately obtain total path attenuation, regional attenuation can be corrected using a multipurpose-microwave-link network based on tomographic reconstruction of attenuation coefficients [37]. The quantitative precipitation estimations from the radar depend on the intensity of echoes reflected by raindrops, but those from the microwave link depend on rainfall attenuation along the path [18].

QPE from weather radar can be affected by many factors. One of the key factors is the rainfall attenuation on the propagation of electromagnetic waves. The rainfall attenuation also effects the radar echo intensity by decreasing. At the long distances, actual values are higher than the reflectivity factors of radar, so this factors do not reflect the actual precipitation distribution [37]. In this section attenuation of radar echoes was corrected with tomographic correction method.

Describing the characterization of the microwave attenuation is really important to correct attenuation. Due to developing the attenuation correction effect, attenuation along the propagation path was measured by many scientists [37]. Lin and Lv [22] suggested to use microwave radiometer to acquire total path attenuation.

The Surface Reference Technique (SRT) is widely preferred technique to measure total path attenuation with space born radar configuration by comparing the acquired echo differences at the rainy and non-rainy areas. In addition to that, Serrar et al [34] proposed to compare radar echo attenuation by taking echo differences in between rainy and non-rainy days, which is called Mountain Reference Technique and clearly refers to SRT. Meneghini et al [26] stated that SRT could be have some restrictions, since the attenuation and reflection of electromagnetic waves are different due to surface fluctuation and humidity.

Determining the signal level of microwave links for the both transmitter and receiver is a way to acquire microwave propagation attenuation. During precipitation period, the microwave attenuates while

it passes through the rain area. Gao et al [11] proposed that to measure this attenuation level, it can be compared the rainy and non-rainy days. This acquired data can be used to show precipitation intensity and correct reflectivity factor of radar. In addition to that, Kramer et al [19] showed the methods to correct radar reflectivity factors for X-band radars by using microwave link, and Kramer and Vervorn [20] stated the algorithms to correct radar reflectivity factors for C-band radar by using microwave link, as well.

In this part, we expanded the region of attenuation correction using multiple microwave links to develop attenuation correction. To obtain the total radar attenuation, we derived the attenuation coefficients of the grids. The method we used is called Computerized Tomography imaging method.

3.1 Theory of The Radar Attenuation Correction

Let $\bar{P}_{r0}$ be the average echo before attenuation, $\bar{P}_r$ be the average echo after attenuation and K_t be the attenuation factor. Then attenuation characteristic can be written as follows

$$\bar{P}_r = \bar{P}_{r0} \times K_t \tag{3.1}$$

Derivation shows that,

$$\frac{d\bar{P}_r}{dr} = -2k_t(r)\bar{P_{r0}} \tag{3.2}$$

where $d\bar{P}_r$ is the attenuation value and $k_t(r)$ is the attenuation coefficient.

The average echo power is the integral solution of (3) from ranges 0 to R.

$$\bar{P}_r = \bar{P_{r0}} \exp(-2\int_0^R k_t(r)dr) \tag{3.3}$$

By using the identity $\log_{10} X = 0.4343(\ln X)$ and the determining the attenuation as $k(r) = 4.343k_t(r)$ in units of $\frac{dB}{km}$, (4)becomes

$$\ln(\frac{\bar{P}_r}{\bar{P_{r0}}}) = -2\int_0^R k_t(r)dr \tag{3.4}$$

It is also derived as follows

$$\bar{P_r} = \bar{P_{r0}} \times 10^{-0.2 \int_0^R k_s dr} \tag{3.5}$$

Comparing (2) and (6), we get that

$$K_t = 10^{-0.2 \int_0^R k_s dr} \tag{3.6}$$

We can create the new equation similar in (2) by using radar reflectivity observation Z_m instead of $\bar{P_r}$ and radar reflectivity of the target Z_r instead of $\bar{P_{r0}}$. Then, we get following equation

$$Z_m = Z_r \times K_t = Z_r \times 10^{-0.2 \int_0^R k_s dr} \tag{3.7}$$

in which K_t is the attenuation factor, R is the distance between radar and the detection target and k_s is attenuation coefficient.

If we take the logarithms of both sides in (8), we get

$$\log Z_m = \log Z_r \times -0.2 \int_0^R k_s dr \tag{3.8}$$

To correct attenuation we need to use radar reflectivity factor. At this point, we need to convert radar reflectivity to radar reflectivity factor. To do this, the following equation can be used

$$z = 10 \log Z \tag{3.9}$$

Then, we have

$$z_r = z_m + 2 \int_0^R k_s dr \tag{3.10}$$

in which z_r is the corrected radar reflectivity factor, z_m is the measured reflectivity factor of radar and k_s is the attenuation coefficient.

3.2 Radon Transform Modeling for Attenuation Coefficients

3.2.1 Reconstruction of Grid Attenuation

To correct attenuation the Computarized Tomography (CT) imaging technology can be used. This technique is based on ray scanning and the attenuation of ray power is acquired through the wave field [37].

The Radon transform and Fourier-Slice theorem are the theoretical basis of CT. We discussed the mathematical theory of the Radon transform and its inverse in the previous parts. In addition to that, we can determine the tomography as the Inverse Radon Transform. In the tomography theory, a function $f(x, y)$ which refers to an image is usually discretized to the pixel level to obtain mean value of $f(x, y)$ in each pixel [37].

Microwave links pass through the precipitation area in the weather radar monitoring field. In a microwave link transmitting end conducts the signal with the frequency, polarization and fixed power and the receiving end acquires the power after attenuation [37].

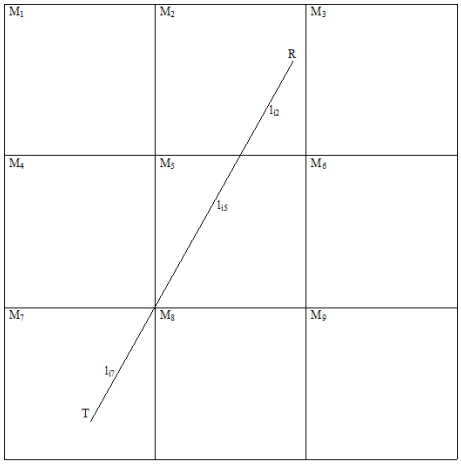

Figure 3.: Diagram of Microwave link in the monitoring area.

Figure represents the attenuation coefficients tomography's schematic diagram for a simulated region. The region was divided into equal meshes M_j $(j = 1, 2, ...)$. Shown microwave link is an example in which T is the transmitting end and R is the receiving end. The link passes through the grids at M_7, M_5 and M_2 with the lengths in the girds is denoted by l_{i7}, l_{i5} and l_{i2}, respectively.

The precipitation attenuation of the microwave link can be formulated as

$$A_i = \sum_{j=1}^{N} l_{ij} k_j \tag{3.11}$$

where l_{ij} is the length of the ith microwave link in the jth mesh, N is the discretized number of meshes [37].

By the power law , it can also be expressed as

$$A_i = a_i R_i^{b_i} l_i \tag{3.12}$$

where R_i is the average precipitation intensity on the ith link, l_i is the length and a_i and b_i are the conversion constants of the ith link [37].

By (3.12), the attenuation of the microwave links can be formulated as

$$A = LK \tag{3.13}$$

where $A = A_i$ is the column vector of the total attenuation, $L = l_{ij}$ is the distance matrix asnd $K = k_j$ is the column vector of the attenuation coefficients. Thus, the following system of equations can be expressed where M is the number of microwave links [37].

$$\begin{aligned} l_{11}k_1 + l_{12}k_2 + \cdots + l_{1N}k_N &= A_1 \\ l_{21}k_1 + l_{22}k_2 + \cdots + l_{2N}k_N &= A_2 \\ &\vdots \\ l_{M1}k_1 + l_{M2}k_2 + \cdots + l_{MN}k_N &= A_M \end{aligned} \tag{3.14}$$

Tomographic model of the attenuation coefficients can be obtained by solving the above linear system(3.14). Solution of the linear equations was explained in details in [12] to acquire the attenuation coefficient [37].

3.3 Numerical Implementation and Regional Attenuation Correction

To correct the regional attenuation, the process is the following

- Creating a joint observation microwave links network and weather radar data
- Matching the observational weather radar and the microwave attenuation data with time and space
- Discretization of the field
- Using reconstruction algorithms to acquire tomographic attenuation coefficients
- Calculating the path attenuation (PA) of the ith link between the radar and the mesh points with the formula

$$(PA)_{ij} = \sum_{i=1}^{M} \sum_{j=1}^{N} k_j d_{ij} \tag{3.15}$$

  where d_{ij} is the length of the ith link between radar and the mesh point through the jth mesh

- Calculating the corrected radar reflectivity factor z_{ij} as follows

$$z_{ij} = z_{m_{ij}} + 2 \times (PA) \tag{3.16}$$

  where $z_{m_{ij}}$ is the measured radar reflectivity factor [37].

To perform the accuracy of the algorithms and techniques, the numerical implementation was simulated. The total distribution of the monitoring area which was discretized with the CT principle was 24×24 km and the area was divided into 3×3 km square grids. In the simulation area there were 30 microwave links. The distances between transmitting and receiving ends were 3 km and the signal frequency was 10 GHz with the vertical polarization.By the International Telecommunication Union (ITU) rainfall model [38] attenuation coefficient $k = 0.00887R^{1.264}$. As tomographic reconstruction models, Simultaneously Iterative Reconstruction Technique and Filtered Backprojection Technique were used and the results were compared.

To analyze the corrections, corellation coefficient, mean square error and mean deviaton were use to define the correction effect

$$\rho = \frac{\sum_{i=1}^{N}(z_{r_i} - \hat{z}_i)(z_i - \hat{z})}{\sqrt{\sum_{i=1}^{N}(z_{r_i} - \hat{z}_i)^2 \sum_{i=1}^{N}(z_i - \hat{z})^2}}$$
$$RMSE = \sqrt{\frac{1}{N}\sum_{i=1}^{N}(z_{r_i} - z_i)^2} \tag{3.17}$$
$$e = \frac{\sum_{i=1}^{N}(z_i - z_{r_i})}{\sum_{i=1}^{N} z_{r_i}}$$

where z_r and z are uncorrected and corrected radar reflectivity factors, respectively and $\hat{z_r}$ and $\hat{z}$ are average radar reflectivity factors, respectively.

Table 1: Comparison of the radar reflectivity

Technique	ρ_{Unc}	ρ_{Cor}	$RMSE_{Unc}$	$RMSE_{Cor}$	e_{Unc}	e_{Cor}
SIRT	0.362	0.7149	12.2328	3.2144	0.2624	0.0144
FBP	0.4823	0.5625	17.65	8.4432	0.3976	0.2311

Table 2: Comparison of the rainfall intensity

Technique	ρ_{Unc}	ρ_{Cor}	$RMSE_{Unc}$	$RMSE_{Cor}$	e_{Unc}	e_{Cor}
SIRT	0.6847	0.9326	24.65	10.871	0.809	0.0467
FBP	0.7129	0.8425	31.283	16.09	0.9174	0.4326

Conclusion In this section, the provided algorithms were analyzed and two different reconstruction techniques were compared. Both SIRT and FBP methods are efficient techniques to improve rainfall attenuation correction. Moreover, results show that the SIRT technique is more effective technique as tomographic correction.

References

[1] Agranovsky,M., Volchkov,V.V., Zalcman, L.A.: *Conical uniqueness sets for the spherical Radon transform*. Bull.Lond.Math.Soc.31, 231-236 (1999).

[2] Antipov, Y.A., Estrada,R., Rubin, B.: *Inversion formulas for spherical means in constant curvature spaces*. J. D'Anal. Math. 118, 623-256 (2012).

[3] Appledorn, C.R., Fang, Y.R., Kruger, R.A., Liu, P.: *Photoacoustic ultrasound (PAUS) reconstruction tomography*. Med.Phys. 22, 1605-1609 (1995).

[4] Batenkov, D., Sarig, N. and Yomdin, Y.: *An algebraic reconstruction of piecewisesmooth functions from integral measurements*. Functional Differential Equations. 19(1-2), 13-30 (2012).

[5] Beltukov, A.: *Inversion of the Spherical Mean Transform with Sources on a Hyperplane*. arXiv:0919.1380v1(2009)

[6] Blu, T., Dragotti, P., Vetterli, M.: *Sampling moments and reconstructing signals of finite rate of innovation: Shannon meets Strang-Fix*. IEEE Trans. Signal Processing. 55(5), 1741-1757(2007)

[7] Cheney, M., Nolan, C.J.: *Synthetic aperture inversion*. Inverse Problems. 18, 221-235(2002)

[8] Elad, M., Golub, G., Milanfar, P.: *Shape from moments - an estimation theory perspective*. IEEE Trans. Signal Processing. 52, 1814-1829(2004)

[9] Finch, D., Patch, S., Rakesh.: *Determining a function from its mean values over a family of spheres*. SIAM J. Math. Anal. 35(5), 1213-1240(2004)

[10] Finch, D., Haltmeier, M., Rakesh.: *Inversion of spherical means and the wave equation in even dimensions*. SIAM J. Appl. Math. 68(2), 392-412(2007)

[11] Gao, T.C., Song, K., Liu, X.C., Yin, M., Liu, L., Jiang, T.S.: *Research on the method and experiment of path rainfall intensity inversion using a microwave link*. Acta Physica Sinica. 64(17), 4301(2015)

[12] Giuli, D., Facheris, L., Tanelli, S.: *Microwave tomographic inversion technique based on stochastic approach for rainfall fields monitoring*. IEEE Transactions onGeoscience and Remote Sensing. vol. 37(5), 25362555(1999)

[13] Golub, G., Gustafsson, B., Milanfar, P., Putinar, M., Varah, J.: *Shape reconstruction from moments: theory, algorithms, and applications*. In Luk, F.T. (ed.) SPIE Proceedings, Advanced Signal Processing, Algorithms, Architecture, and Implementations X. 4116, 406-416(2000)

[14] Gravin, N., Lasserre, J., Pasechnik, D.V., Robins, S.: *The inverse moment problem for convex polytopes*. Discrete and Computational Geometry. 48(3), 596-621(2012)

[15] Haltmeier, M.: *Inversion of circular means and the wave equation on convex planar domains*. Comput. Math. Appl. 65(7), 1025-1036(2013)

[16] Haltmeier, M.: *Universal inversion formulas for recovering a function from spherical means*. SIAM J. Math. Anal. 46(1), 214-232(2014)

[17] Karl, W.C., Milanfar, P., Verghese, G.C., Willsky, A.S.: *Reconstructing polygons from moments with connections to array processing*. IEEE Trans. Sign. Process. 43(2), 432-443(1995)

[18] Kim, M., Kwon, B.H.: *Rainfall Detection and Rainfall Rate Estimation Using Microwave Attenuation*. Atmosphere. 8, 287-309(2018)

[19] Kramer, S., Verworn, H.R., Redder, A.: *Improvement of X-band radar rainfall estimates using a microwave link*. Atmospheric Research. 77(1-4), 278299(2005)

[20] Kramer, S., Verworn, H.R.: *Improved C-band radar data processing for real time control of urban drainage systems*. Proceedings of the 11th International Conference on Urban Drainage. 110, Hydro International, North Somerset, UK(2008)

[21] Kunyansky, L.A.: *Explicit inversion formulae for the spherical mean Radon transform*. Inverse Probl. 23(1), 373-383(2007)

[22] Lin, H., Lv, D.R.: *Comparisons and combined uses of radar and radiometer in the remote sensing of rainfall distributions*. Chinese Journal of Atmospheric Sciences. 4(1), 3039(1980)

[23] Louis, A.K., Quinto, E.T.: *Local tomographic methods in Sonar*. In: Surveys on Solution Methods for Inverse Problems. 147-154. Springer, Vienna (2000)

[24] Maravic, I., Vetterli, M.: *Exact sampling results for some classes of parametric nonbandlimited 2-D signals*. IEEE Trans. Signal Process. 52(1), 175-189(2004)

[25] Maravic, I., Vetterli, M.: *Sampling and reconstruction of signals with finite rate of innovation in the presence of noise*. IEEE Trans. Signal Process. 53(8 part 1), 2788-2805(2005)

[26] Meneghini, R., Iguchi, T., Kozu, T.: *Use of the surface reference technique for path attenuation estimates from the TRMM precipitation radar*. Journal of Applied Meteorology. 39(12), 20532070(2000)

[27] Natterer, F.: *Photo-acoustic inversion in convex domains*. Inverse Probl. Imaging 2, 315-320(2012)

[28] Patch, S.K.: *Thermoacoustic tomography - consistency conditions and the partial scan problem*. Phys. Med. Biol. 49, 111(2004)

[29] Rubin, B.: *Introduction to Radon transforms: With elements of fractional calculus and harmonic analysis*. Encyclopedia of Mathematics and its Applications. Cambridge University Press (2015)

[30] Rubin, B.: *Reconstruction of functions on the sphere from their integrals over hyperplane sections*. arXiv:1810.09017(2018)

[31] Salman, Y.: *Recovering finite parametric distributions and functions using the spherical mean transform.*. Anal. Math. Phys. 8(3), 437-463(2018)

[32] Sarig, N., Yomdin, Y.: *Signal Acquisition from Measurements via Non-Linear Models*. C. R. Math. Rep. Acad. Sci. Canada. 29(4), 97-114(2007)

[33] Semyanitsky, V.I.: *On some integral transformations in Euclidean space*. Dokl. Akad. Nauk SSSR. 134, 536539(1960)

[34] Serrar, S., Delrieu, G., Creutin, J.D., Uijlenhoet, R.: *Mountain reference technique: use of mountain returns to calibrate weather radars operating at attenuating wavelengths*. Journal of Geophysical Research: Atmospheres. 105(2), 22812290(2000)

[35] Volchkov, V.V.: *Integral geometry and convolution equations*. Kluver, Dordrecth(2003)

[36] Wang, L.V., Xu, M.: *Universal back-projection algorithm for photoacoustic computed tomography*. Phys. Rev. E 71(1),016706(2005)

[37] Xue, Y., Liu, X.C., Gao, T.C., Yang, C., Song, K.: *Regional Attenuation Correction of Weather Radar Using a Distributed Microwave-Links Network*. In: Advances in Meteorology (2017)

[38] Zhao, Z.W., Zhang, M.G., Wu, Z.S.: *Analytic specific attenuation model for rain for use in prediction methods*. Journal of Infrared, Millimeter, and Terahertz Waves. 22(1), 113120(2001)

Appendix A

Matlab Codes

FBP and SIRT Codes with Weighted Matrix

```
function Reconstruction
%Load image here
figure, subplot (3,2,1),
imshow(Image)
subplot(2,3,1);
imagesc(Image);
title('Original Image');

% padding to the image with zeros to not to lose anything while
    rotating.
[Length, Width] = size(Image);
Diag = sqrt(Length^2 + Width^2);
LengthPad = ceil(Diag - Length) + 2;
WidthPad = ceil(Diag - Width) + 2;
padImage = zeros(Length+LengthPad, Width+WidthPad);
padImage(ceil(LengthPad/2):(ceil(LengthPad/2)+Length-1), ...
     ceil(WidthPad/2):(ceil(WidthPad/2)+Width-1)) = Image;
%
frequency= 0.5;
theta = 1:frequency:180;
subplot(2,3,2)
```

```
% Creating Sinogram
```

```
Sinogram = radon(Image,theta);
imagesc(Sinogram);
title('Sinogram')
subplot(2,3,3)

% Backprojection Procedure
PP = size(Sinogram,1);%Number of Parallel Projections
AP  = length(theta);%Number of Angular Projections
theta = (pi/180)*theta;
BPI = zeros(PP,PP);%Setup backprojected image
MI = ceil(PP/2);%Middle index of projections
[x1,y1] = meshgrid(ceil(-PP/2):ceil(PP/2-1));%new coordinates

 % Filtering Procedure 'RamLak'
if mod(PP,2) == 0
    FS= 2*floor(1 + PP);%filter size
else
    FS = 2*floor(PP);
end
    filter = zeros(1, FS);
    filter(1:2: FS) = -1./([1:2: FS].^2 * pi^2);
    filter = [fliplr(filter) 1/4 filter];

% Projection loops
for i = 1:AP
    rotCoords = round(MI + x1*sin(theta (i)) + y1*cos(theta(i)));
    indices   = find((rotCoords > 0) & (rotCoords <= PP));
    newCoords = rotCoords(indices);
    filteredProfile = conv(Sinogram(:,i),filter,'same');
    BPI(indices) =  BPI(indices) + filteredProfile(newCoords)./AP;
```

```
32      imagesc(BPI);
33      title('BPI');
34      drawnow
35
36  end
37
38  MI = floor(size(BPI,1)/2) + 1;%find the middle index of the
        projections
39
40
41  %Pre-filter for the freq domain
42  [x1,y1] = meshgrid(1-MI:size(BPI,1)- MI);
43  ramp_filter = sqrt(x1.^2 + y1.^2);
44
45  %Fourier transformation
46  Rec = fftshift(fft2(BPI));
47
48  % Filtering for the freq domain
49  Rec = Rec.* ramp_filter;
50
51  % inverse fourier transformation
52  Rec = real(ifft2(ifftshift(Rec)));
53
54  RI= mat2gray(Rec);
55  subplot(2,3,4);
56  imshow(RI);
57  title('FBI');
```

```
1  % Creating Sinogram
2  Sinogram = radon(Image,theta);
3  imagesc(Sinogram);
```

```
4  title('Sinogram')
5  subplot(2,3,3)
6
7  % Backprojection Procedure
8  PP = size(Sinogram,1);%Number of Parallel Projections
9  AP  = length(theta);%Number of Angular Projections
10 theta = (pi/180)*theta;
11 BPI = zeros(PP,PP);%Setup backprojected image
12 MI = ceil(PP/2);%Middle index of projections
13 [x1,y1] = meshgrid(ceil(-PP/2):ceil(PP/2-1));%new coordinates
14
15  % Filtering Procedure 'RamLak'
16 if mod(PP,2) == 0
17     FS= 2*floor(1 + PP);%filter size
18 else
19     FS = 2*floor(PP);
20 end
21     filter = zeros(1, FS);
22     filter(1:2: FS) = -1./([1:2: FS].^2 * pi^2);
23     filter = [fliplr(filter) 1/4 filter];
24
25 % Projection loops
26 for i = 1:AP
27     rotCoords = round(MI + x1*sin(theta (i)) + y1*cos(theta(i)));
28     indices   = find((rotCoords > 0) & (rotCoords <= PP));
29     newCoords = rotCoords(indices);
30     filteredProfile = conv(Sinogram(:,i),filter,'same');
31     BPI(indices) =  BPI(indices) + filteredProfile(newCoords)./AP;
32     imagesc(BPI);
33     title('BPI');
```

```
34      drawnow
35
36  end
37
38  MI = floor(size(BPI,1)/2) + 1;%find the middle index of the
        projections
39
40
41  %Pre-filter for the freq domain
42  [x1,y1] = meshgrid(1-MI:size(BPI,1)- MI);
43  ramp_filter = sqrt(x1.^2 + y1.^2);
44
45  %Fourier transformation
46  Rec = fftshift(fft2(BPI));
47
48  % Filtering for the freq domain
49  Rec = Rec.* ramp_filter;
50
51  % inverse fourier transformation
52  Rec = real(ifft2(ifftshift(Rec)));
53
54  RI= mat2gray(Rec);
55  subplot(2,3,4);
56  imshow(RI);
57  title('FBI');
```

```
1  %Pre-filter for the freq domain
2  [x1,y1] = meshgrid(1-MI:size(BPI,1)- MI);
3  ramp_filter = sqrt(x1.^2 + y1.^2);
4  %Fourier transformation
5  Rec = fftshift(fft2(BPI));
```

```
% Filtering for the freq domain
Rec = Rec.* ramp_filter;
% inverse fourier transformation
Rec = real(ifft2(ifftshift(Rec)));
RI= mat2gray(Rec);
subplot(2,3,4);
imshow(RI);
title('FBI');
end
```

```
%Weighted matrix codes

function W = Weight(x,y,z,t)
x = [0:x-1] - (x-1)/2;
y = (-1)*([0:y-1] - (y-1)/2);
pixel = length(x);
theta = [0:t-1]'/t * pi;
t = cos(theta) * x' + sin(theta) * y';
t = t + (z+1)/2;
a = floor(t); % Find left bins of projected pixel centers.
lb = 1 - (t-a); % left bins
rb = 1-lb; % right bins
n_c = x * y; %number of column
ri = a + [0:t-1]'*z*ones(1,pixel); % row_indices
cj = find(fn(:))';
cj = cj(ones(1,t),:); % column indices
value=a(:) >= 1
W = sparse(ri,cj), lb, z*t, n_c); %Sparse weighted matrix

% SIRT codes

```

```
22 function I = sart(W,f,p,iteration)
23 I= zeros(f,1);
24 Wt = W';
25 C = sum(Wt);
26 R = sum(W);
27 for k = 1:iteration
28 q = W*f;
29 A = (p-q)./R;
30 B = Wt * A;
31 f = f + (B ./ C);
32 I = f;
33 end
34 I=reshape(I,n,n);
35 I=I';
```